Dedicated to Academician Aureliu Săndulescu's 80th Anniversary

NUCLEAR STRUCTURES OF THE NEUTRON-RICH NUCLEI AROUND A=120

Y.X. LUO[1,2], S.H. LIU[1], J.H. HAMILTON[1], A.V. RAMAYYA[1], J.O. RASMUSSEN[2], J.K. HWANG[1], N.T. BREWER[1], S.J. ZHU[3]

[1]Physics Department, Vanderbilt University, Nashville, TN 37235, USA
[2]Lawrence Berkeley National Laboratory, Berkeley, CA 94720, USA[3]Tsinghua University, Beijing 100084, People's Republic of China

Received September 30, 2011

Analysis of high statistics triple coincidence fission γ data from ^{252}Cf at Gammasphere including angular correlations yielded well-expanded high-spin level schemes with more complete and reliable spin/parity assignments for ^{118,120,122}Cd and ^{114,115}Rh. Both the quasi-particle/hole couplings and quasi-rotational degrees of freedom are implied to play roles in these Cd isotopes. Evidence for triaxial shapes and octupole components in the Cd isotopes is presented. These Cd isotopes may have triaxial deformations implied by the Frauendorf SCTAC model calculations. High-spin level schemes of ^{114,115}Rh have been established for the first time. The existence of a relatively large signature splitting and an yrare band shows typical features of a triaxially deformed nucleus. This paper is dedicated to our long-time colleague Prof. Aureliu Săndulescu on the occasion of his 80th birthday.

Key words: Neutron-rich nuclei, Spontaneous fission, Triaxiality.

1. INTRODUCTION

The neutron-rich nuclei with A > 114 are intermediate between the spherical doubly magic Sn isotopes and the strongly deformed heavy Zr and Mo nuclei. The neutron-rich Cd isotopes with Z=48 are of special interest since they are very close to the Z=50 major shell. There has been much study of the quasi-collectivity in these nuclei and its evolution with spins and neutron numbers. For the nuclei in this region the $\upsilon h_{11/2}$ orbital is close to the Fermi surface and the deformation-driving effects could play an important role. Likewise, the nearly-filled proton orbitals, $\pi g_{9/2}$ and $\pi p_{1/2}$, can have an influence.

The earliest information on low-lying excited states of the neutron-rich Cd isotopes in this region was obtained in (d,p) reactions [1, 2]. Then further work on these states in the nuclei were made by means of measurements of β decay of Ag

isotopes produced in thermal neutron-fission in uranium target and separated by OSIRIS on-line mass separator [3,4]. The ratios of the 4^+ to 2^+ excitations were found to rise slightly from ^{114}Cd to ^{116}Cd but then stay constant as 2.38 in ^{116}Cd, ^{118}Cd and ^{120}Cd. B(E2; $2_2^+ \rightarrow 0^+$)/ B(E2; $2_2^+ \rightarrow 2_1^+$) were deduced to be 0.03, 0.04, 0.07 and 0.09 in ^{114}Cd, ^{116}Cd, ^{118}Cd and ^{120}Cd, respectively. All these values are small implying vibrational character for low-lying states in these Cd isotopes [5]. More detailed work on low-lying states of ^{118}Cd was done at separator TRISTAN by Aprahamian et al., and a set of five closely spaced levels at ~2 MeV was observed in the nucleus, which were interpreted as a nearly harmonic three-phonon excitation, and provided strong evidence that well-developed vibrational structure can indeed exist [6]. Fast timing measurements by means of β-γ-γ coincidences were carried out by Mach *et al.* to measure lifetimes of low-lying states [7]. Quasi-collective character of the low-lying states in these Cd isotopes were implied by the essentially constant B(E2; $0_1^+ \rightarrow 2_1^+$) values, about six single-particle units, in ^{116}Cd, ^{118}Cd and ^{120}Cd. Vibrational and intruder structure of these nuclei were proposed. Then Wang *et al.* [8] established extended decay schemes of ^{118}Ag and ^{120}Ag to ^{118}Cd and ^{120}Cd using β-γ and γ-γ coincidences following on-line mass separations, which supported the coexistence of quadrupole anharmonic vibration and proton particle –hole intruder excitations in the Cd isotopes. The onset of isomers in $^{125\text{-}128}$Cd was observed by using fragmentations of 120 MeV/nucleon ^{136}Xe beam [9]. Evidence for odd-parity side-bands in ^{112}Cd [10,11], ^{108}Cd [12], ^{114}Cd [13], ^{116}Cd [14] and ^{110}Cd [15] were found.

Preliminary high-spin level schemes of the Cd isotopes were established by measurements of prompt γ rays from heavy-ion fusion-fission reactions at Gammasphere by Fotiades *et al.* [20,21]. The ground bands of ^{114,116,118,120}Cd were extended up to excitations ~ 5.5 MeV. Almost at the same time as the above-mentioned work, Buforn et al. reported the high-spin level schemes of ^{113,114,115,116}Cd with side bands observed in each of the four Cd isotopes, also using heavy-ion fusion-fission reactions at Eurogam2 [22]. Buforn et al. also carried out Hartee-Fock theoretical calculations for ^{110,112,114,116}Cd showing prolate minima. They suggested weakly prolate deformations in this mass region especially for the odd N Cd isotopes. Xiao et al. studied the yrast states of ^{116,118,120}Cd and tentatively suggested odd-parity bands in the even-N Cd isotopes [24]. Nelson *et al.* of our collaboration proposed in his senior thesis new level schemes of ^{120,122}Cd with side bands observed in ^{120}Cd [25]. He made spin/parity assignments for levels in ^{120,122}Cd based on gamma-gamma angular correlation measurements. However, except for ^{120}Cd, the preliminary level schemes of Cd isotopes, mainly consisting of the ground band (for even-N Cd isotopes) were not expanded enough to provide information for further determination of the nuclear structure of the Cd isotopes. The present paper reports the new high-spin level schemes of ^{118,120,122}Cd, which were considerably expanded, based on the high-statistics triple and higher-fold coincidence data accumulated by detecting prompt γ rays from spontaneous fission of ^{252}Cf at Gammasphere. It is generally true (except for β decay from high-spin parents) that more detailed exploration of the high spin yrast and near-yrast

spectroscopy of the neutron-rich nuclei was not realized until such high-statistics accumulations of prompt fission γ rays were made with the advent of large γ–detector arrays [26, 27]. Based on the expanded level schemes of the Cd isotopes, the spin/parity assignments, nuclear structure and band-patterns of the observed levels were investigated and reported [28].

The Z = 45 neutron-rich Rh isotopes are five protons below the 50 proton closed shell and midway between the 50 and 82 neutron major shells. In this region, nuclei are characterized by shape coexistence and shape transitions, including triaxial shapes [29, 30]. The active proton orbitals, near the top of the $\pi g_{9/2}$ subshell, drive the nuclear shape towards oblate deformations, while the neutron Fermi levels, below or near the bottom of the $\nu h_{11/2}$ sub-shell, drive the shape to prolate deformations. These tendencies have been observed in the yrast bands of odd-Z and odd-N nuclei which are built on the $\pi g_{9/2}$ and $\nu h_{11/2}$ orbitals. Shape coexistence and transitions in even-Z nuclei in this region have been studied experimentally [26]. The proton orbitals originating from the $g_{9/2}$ sub-shell are influenced by the triaxial nuclear deformation. The appearance of triaxial deformations and soft shape transitions were found in nuclei of Z > 40 [26, 31–35]. Odd-odd Rh isotopes are of great interest in that a remarkable similarity in their high-spin, negative-parity yrast states was seen through a large range of neutron numbers from 59 (^{104}Rh) to 67 (^{112}Rh) [32, 36-38]. The spin-parity of the band-head is 6^- with a 7^- intermediate state from N = 59 to N = 65 and then the band-head becomes 7^- at N = 67 (^{112}Rh). These ΔI = 1, negative-parity yrast bands originating from the coupling of a proton in the $g_{9/2}$ orbital with a strongly aligned $h_{11/2}$ neutron are present at low and moderate excitations. Thus, it is worth exploring the structure of Rh isotopes in the more neutron-rich region with N > 68. Low-lying states in ^{114}Rh (N = 69) were observed in decay studies [39]. However, no high-spin states in ^{114}Rh had been reported before this work. Here, we describe a high spin level scheme of ^{114}Rh reported for the first time with the observation of signature inversion observed in its yrast band [40].

Our previous systematic studies of neutron-rich, odd-even Y, Nb, Tc, and Rh (Z = 39, 41, 43, 45) isotopes indicated a shape transition from axial symmetry with large quadrupole deformations in ^{99,101}Y to a deformed shape with large triaxiality in ^{107,109,111}Tc and ^{111,113}Rh [32-35]. In a ground state with Z = 45, the valence protons occupy holelike states in the Z = 50 closed shell, with a main configuration $\pi 1g_{9/2}{}^5$. The valence neutrons occupy mainly particlelike states in the 50–82 shells. Due to the proton-neutron interaction, the nucleus is deformed, with a tendency to triaxiality. Rotational bands built on $\pi g_{9/2}$, $\pi p_{1/2}$, and $\pi(g_{7/2}d_{5/2})$ subshells have been observed in odd-even $^{107-113}$Rh [32, 41, 42]. The existence of an yrare band built on an $11/2^+$ excited state and a large signature splitting in the yrast band in ^{107,109,111,113}Rh provides evidence for triaxiality,which has been confirmed by theory. Theoretical calculations based on the rigid triaxial rotor plus particle (RTRP) model provideda reasonable fit to excitation energies and branching ratios of the yrast bands and the collective yrare bands as well as to the signature splittings in the yrast bands of ^{111,113}Rh at near-maximum triaxiality with $\gamma = 28^\circ$

[32], larger than $\gamma = 23^{\circ}$ for ^{107}Rh [41]. Thus, it is of interest to study the structure evolution of odd-even Rh to the more neutron-rich region. Low-lying excited states in ^{115}Rh were reported in Ref. [43] through β-decay studies of ^{115}Ru, and $7/2^{+}$ was assigned to the ground state of ^{115}Rh [44]. Here, we describe the first high-spin level scheme of the very neutron-rich nucleus ^{115}Rh (N = 70) [45].

2. EXPERIMENT AND DATA ANALYSIS

Our experiment was carried out at Gammasphere in the Lawrence Berkeley National Laboratory. A ^{252}Cf source of 62 μCi, sandwiched between two 10 mg/cm^2 Fe foils, was placed in an 8-cm-polyethylene ball centered in the Gammasphere [46] which had 101 Compton-suppressed Ge detectors active. Over 5.7×10^{11} triple and higher-fold events were accumulated. The Radware cube three-dimensional histogram and less-compressed cube with one-third less compression [47] based on these high statistics and high quality triple coincidence data provided the key conditions to explore the level schemes of the Cd and Rh isotopes. The identification of a new transition in the Cd and Rh isotopes was based on cross-checking the coincident relationships with its low-lying known transitions and with those of its complementary fission partners Sn and I isotopes. Transition energies, branching ratios of levels were determined by peak-fittings [47] with proper background subtractions.

2.1. ^{118,120,122}Cd

Fig.1 shows an example of many cross-checking double-gated, triple-coincidence spectra in the data analysis for ^{118}Cd, ^{120}Cd and ^{122}Cd.

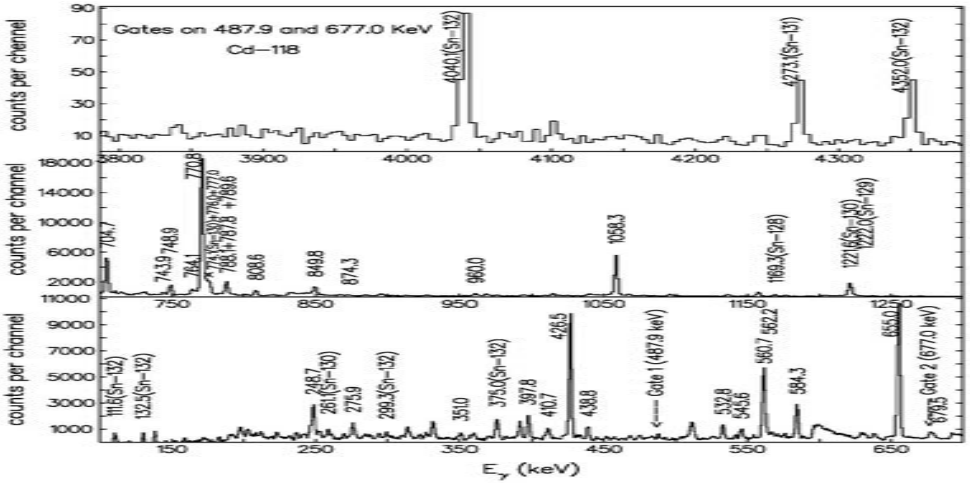

Fig. 1 – Spectrum gated on 487.9 and 677.0 keV transitions in ^{118}Cd [28].

Based on coincidence relationships and relative intensities of the transitions new level schemes of ^{122,120,118}Cd are established, as shown in Figs. 2, 3 and 4, respectively. The ground band of ^{118}Cd reported in [20, 21] was confirmed up to the 5326.0 keV, (16^+) level. A total of 13 new transitions and five side-bands were observed in the present fission work, forming a considerably expanded high-spin level scheme of ^{118}Cd as shown in Fig. 4. In the level scheme of ^{118}Cd reported in [8] the authors proposed a 2182.1 keV level which is fed by an 849.8 keV transition and depopulated by a 246.2 keV transition which feeds the 1935.7 keV 6^+ level. However, our data analysis shows that the 849.8 keV transition feeds the 1935.7 keV level and depopulates the 2785.5 keV level. The 2182.1 keV level does not exist in our work. A total of 22 new transitions with two side-bands observed in ^{120}Cd by Nelson [25] and our collaboration [28] are described here. Our considerably expanded new level scheme of the nucleus is shown in Fig. 3. Gamma transition branching ratios in ^{118,120}Cd are shown in Table 1.

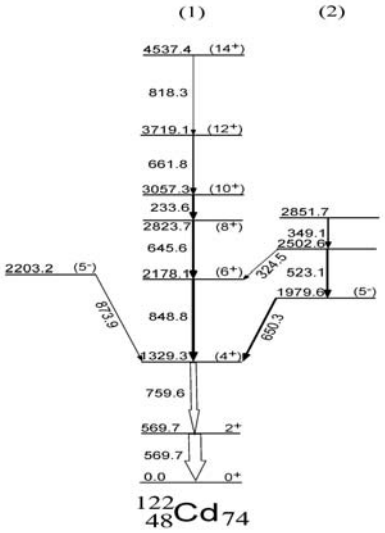

Fig.2 – Level scheme of ^{122}Cd[25,28].

Angular correlation measurements, as described by Daniel *et al.* [48], anddecay patterns were utilized to assign spins/parities to the newly observed levels in ^{118,120,122}Cd (see Figs. 2, 3 and 4). The theoretical A_2, A_4 and δ were taken from compilations [49, 50]. Possible spin changes and multipolarities were determined for those transitions. In [25] Nelson *et al.* of our collaboration reported angular correlations for the (6^+) – 4^+– 2^+ cascade (829.7 – 697.6 keV) and then (8^+) – 6^+– 4^+ cascade (852.8 – 829.7 keV) in the ground band of ^{120}Cd. In the former we had A_2 = 0.120 (16), A_4 = -0.005 (24); in the latter A_2 = 0.098(28), A_4 =0.010 (42). The theoretical values for stretched E2 cascades are A_2 = 0.102, A_4 = 0.009, in good agreement with the above A_2 and A_4 values, respectively, implying stretched E2 character for the 829.7 and 852.8 keV transitions. Spin/parities of 6^+ and 8^+ are thus definitely assigned to the 2033.2 keV and 2886.0 keV level, respectively. We feel it reasonable to assign stretched E2 to all the in-band transitions in ground bands of ^{118,120}Cd except for those quasi-particle states below the 5^- level of band 2 in ^{118,120}Cd.Fig. 5 shows the angular correlations for the 677.0 – 1058.3 keV cascade in ^{118}Cd, the 677.0 keV transition being known as a stretched E2. A spin change $\Delta I = 1$ and pure dipole is assigned to the 1058.3 keV transition, with $\Delta I = 0$ being excluded. For the 5- 4(2) - 2 cascade (677.0 – 1058.3 keV) with 5 – 4 being pure dipole, one has theoretical values A_2 = -0.071, A_4 = 0.0, in good agreement

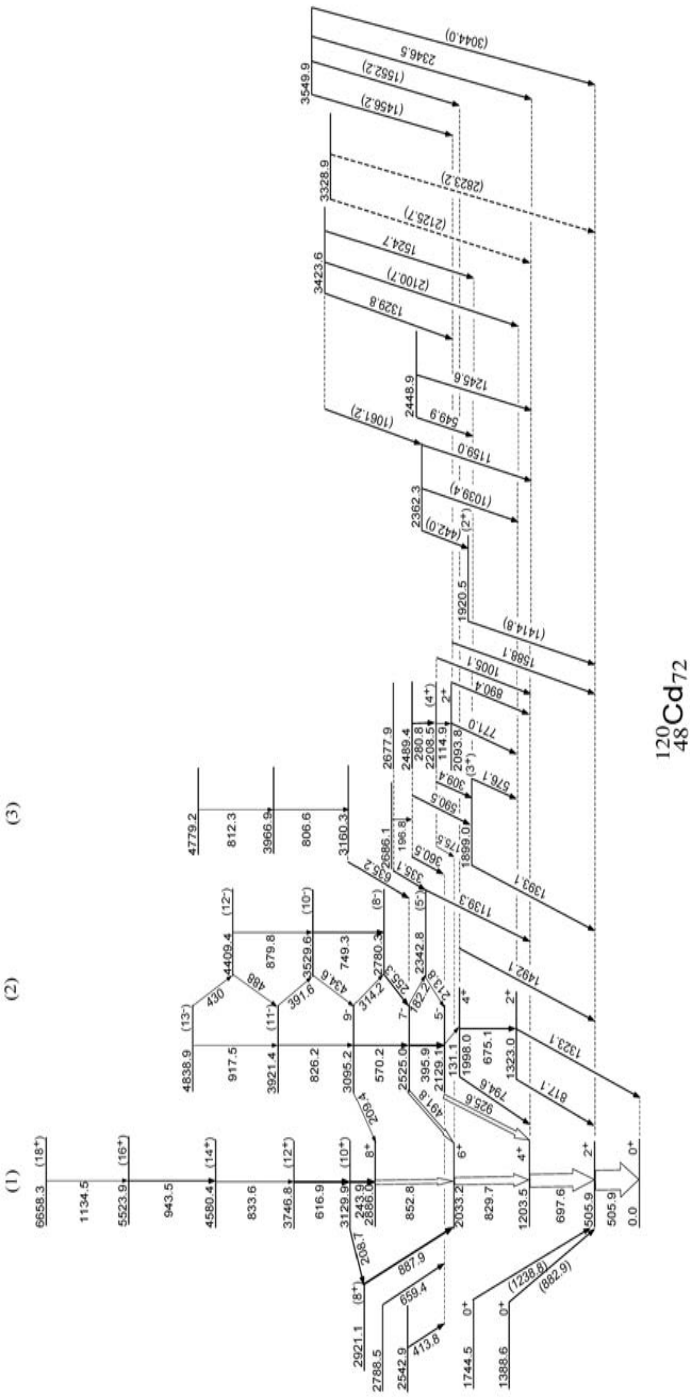

Fig. 3 – Level scheme of ^{120}Cd [25, 28].

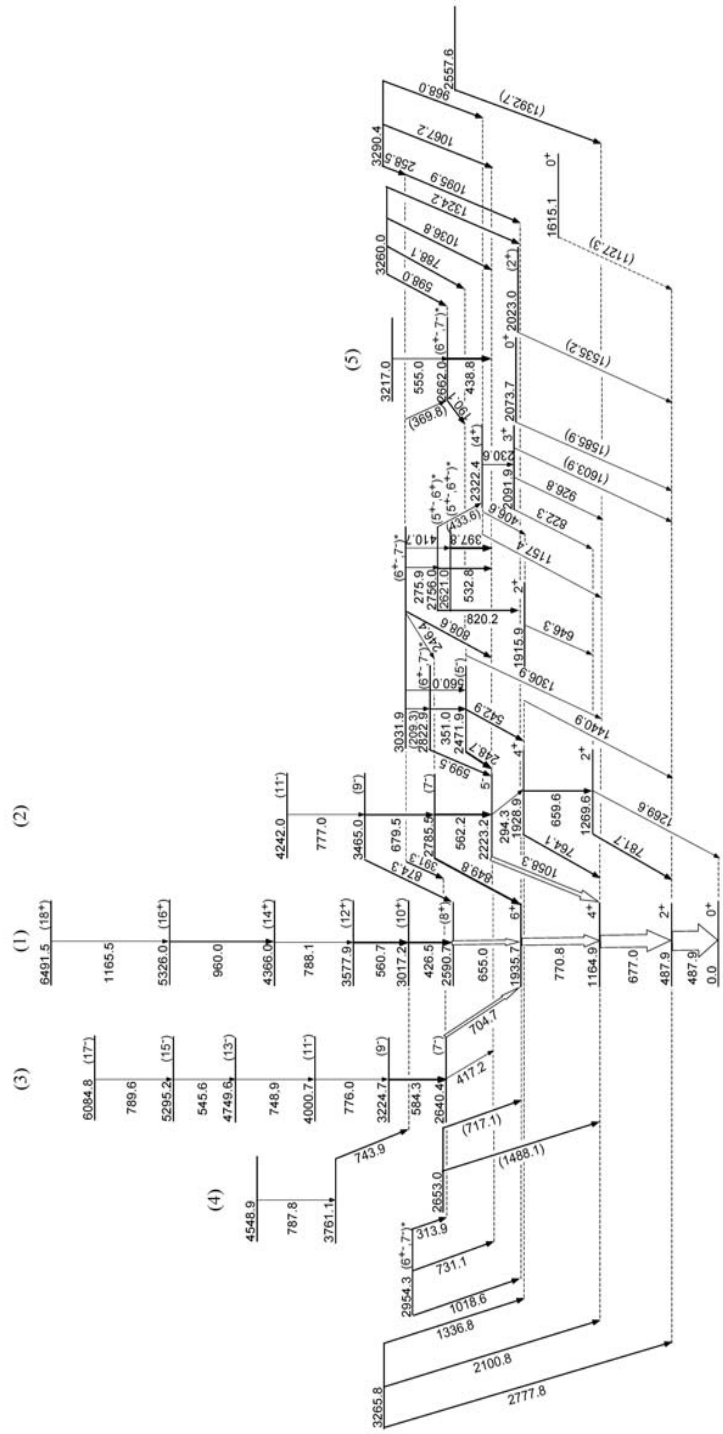

Fig. 4 – Level scheme of ^{118}Cd [28].

with the experimental A_2, A_4 values. These are the only possible spins, multipolarities in agreement with the experiment. The $\Delta I = 1$ and pure dipole assignment to the 1058.3 keV transition and the decay path of the levels led to an assignment of 5^- to the 2223.2 keV level. The in-band transitions in band 2 are believed to be of stretched E2 character by virtue of their large transition energies and branching transitions (presumably E1) going to the ground band. Spin/parity (7^-), (9^-) and (11^-) are thus assigned to the 2785.5, 3465.0 and 4242.0 keV levels, respectively. In the β decay study the 1269.6 keV level was assigned as 2^+, and the 1928.9 keV level as 4^+, which implies an E1 for the 294.3 keV transition between the 2223.2 keV, 5^- and the 1928.9 keV, 4^+ level.

Table 1

Gamma transition branching ratios from levels with spins 0, 2, 3, 4, 5, and 6 in ^{118,120}Cd [28]

Nucleus	Level (keV)	Spin/parity	Decaying E_γ (keV)	I_γ	Spin/parity of final state	Nucleus	Level (keV)	Spin/parity	Decaying E_γ (keV)	I_γ	Spin/parity of final state
^{118}Cd	0.0	0^+_1				^{120}Cd	0.0	0^+_1			
	1285.8	0^+_2	798.0	weak	2^+_1		1388.6	0^+_2	882.9	0.8	2^+_1
	1615.1	0^+_3	1127.3	weak	2^+_1		1744.5	0^+_3	1238.8	0.4	2^+_1
	2073.7	0^+_4	1585.9	weak	2^+_1		505.7	2^+_1	505.7	100	0^+_1
	487.8	2^+_1	487.8	100	0^+_1		1322.8	2^+_2	817.0	14.4	2^+_1
	1269.5	2^+_2	781.7	3.3	2^+_1				1322.9	7.5	0^+_1
			1269.5	2.3	0^+_1		1920.5	(2^+_3)	1414.80	2.8	2^+_1
	2023.0	(2^+_3)	1535.2	0.3	2^+_1				1920.6	Weak	0^+_1
	2091.6	3^+	822.1	0.7	2^+_2		2093.8	2^+_4	771.1	3.3	2^+_2
			926.6	0.8	4^+_1				890.40	2.7	4^+_1
			1603.6	1.4	2^+_1				1588.1	7.1	2^+_1
	1164.9	4^+_1	677.1	88.5	2^+_1		1899.0	(3^+)	576.1	3.0	2^+_2
	1929.1	4^+_2	659.6	4.5	2^+_2				1393.4	4.9	2^+_1
			764.3	2.5	4^+_1		1203.2	4^+_1	697.5	100	2^+_1
			1441.3	2.9	2^+_1		1997.9	(4^+_2)	675.0	2.6	2^+_2
	2322.4	(4^+_3)	230.9	0.7	3^+				794.7	2.3	4^+_1
			406.6	0.8	(2^+_3)				1492.3	1.8	2^+_1
			1157.4	4.0	4^+_1		2208.5	4^+_3	115.0	0.7	2^+_4
	2223.3	5^-_1	294.2	3.1	4^+_2				175.7	1.5	6^+
			1058.4	37.0	4^+_1				309.4	5.9	(3^+)
	2471.8	(5^-_2)	248.5	7.6	5^-_1				1005.2	7.2	4^+_1
			542.7	1.6	4^+_2		2128.9	5^-_1	131.1	1.9	(4^+_2)
			1306.9	0.5	4^+_1				925.6	55.1	4^+_1
	1935.9	6^+	770.8	22.3	4^+_1		2342.5	5^-_2	213.8	8.0	5^-_1
									1139.3	5.8	4^+_1
							2032.8	6^+	829.6	20.4	4^+_1

Angular correlations for the 704.7 – 770.8 keV cascade in ^{118}Cd were measured, too. The 770.8 keV transition is known as a stretched E2. A ΔI = 1 and

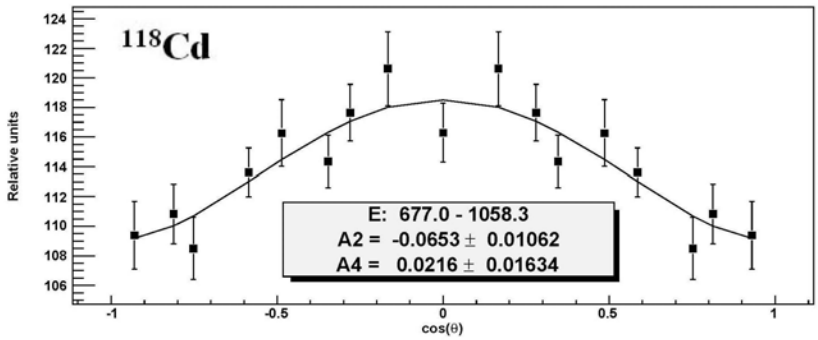

Fig. 5 – Angular correlations for 677.0 – 1058.3 keV cascade in 118Cd. Pure dipole is assigned to the 1058.3 keV transition[28].

pure dipole is assigned to the 704.7 keV transition, with ΔI = 0 being excluded. Theoretical angular correlations of 6(1,2) – 6(2) – 4 cascade (704.7 – 770.8 keV) were checked assuming the 704.7 keV transition to be pure dipole, pure quadrupole or mixed transition with different δ. All these alternative theoretical A_2 and/or A_4 values are in disagreement with the experimental values, so a ΔI = 0 assignment was excluded. Considering the angular correlations and the decay pattern, 7^- is assigned to the 2640.4 keV level in ^{118}Cd. Since all the in-band transitions in band 4 have large transition energies and lack of branching transitions, they are believed to be stretched E2, and spins of (9^-), (11^-), (13^-), (15^-) and (17^-) are assigned to the above levels, respectively. Note the apparent band doubling of bands (2) and (3), though there are not the branching transitions into ground band from band (3) that there are for band (2), and band (3) has no 5^- counterpart.The angular correlation for the 697.6 – 925.6 keV cascade in ^{120}Cd was measured. The 697.6 keV transition has been known as a stretched E2. Properties of ΔI =1 and pure dipole are assigned to the 925.6 keV transition, with ΔI = 0,2 excluded.

More angular correlations were tried with coincidence with a lower transition, 505.9 keV, known also as a stretched E2 in the band 1. Experimental A_2 = -0.087 (20), A_4 = -0.023 (31), in good agreement with theoretical A_2 = -0.071, A_4 = 0.0, δ = 0.0, to give a pure dipole assignment to the 925.6 keV transition**.** An assignment of 5^- is thus given to the 2129.1 keV level. The angular correlation was also determined for the 829.7 – 491.8 keV cascade with the former being known to be stretched E2, giving experimental A_2 = -0.0953 (35), A_4 = -0.021 (54). For a pure dipole in a 7 – 6(2) – 4 cascade, theoretical A_2 = -0.071, A_4 = 0.0, δ = 0.0, in agreement with the experimental values. No agreement can be achieved between experimental and theoretical A_2 for any other spins or multipolarities. The

assignment as 7^- for the 2525.0 keV level and that as 5^- for the 2129.1 keV level confirm the proposed stretched E2 character for the 395.9 keV in-band transition in the band 2. In order to assign spin/parity to one more level in the above-band (band 2) in ^{120}Cd, the angular correlation for 491.8 – 570.2 keV cascade was determined (see the level scheme of ^{120}Cd in Fig. 3). For a stretched E2 – pure dipole 9(2) – 7 – 6 cascade, theoretical values of A_2 = -0.118, A_4 = 0.0, $\delta = 0.00012$, are in good agreement with the experimental A_2 = -0.123 (11), A_4 = 0.013 (18), implying a stretched E2 for the 570.2 keV transition. No agreement is found for any other assignments. The correlations of the 491.8 – 570.2 keV cascade not only indicate stretched E2 for the 570.2 keV transition, implying a 9^- assignment to the 3095.2 keV level in the band 2, but also support the 7^- assignment to the 2525.0 keV level. As discussed above for ^{118}Cd, values of (11^-) and (13^-) are assigned to the 3921.4 and 4838.9 keV level, and (8^-) , (10^-) and (12^-) are assigned to the 2780.3, 3529.6 and 4409.4 keV level, respectively. No transition was observed between the 2780.3 and 2129.1 keV level, which supports the assignment of (8^-) to the 2780.3 keV level (Fig. 3).

2.2. ^{114,115}Rh

From coincidence spectra double-gated on transitions in ^{134}I and ^{135}I, two new transitions of energies 195.9 and 278.1 keV were seen, along with those previously known strong transitions in ^{111,112,113}Rh [32, 37]. The spectra gated on the new 195.9-keV transition and the 952.4-keV transition in ^{134}I as well as the 1133.8-keV transition in ^{135}I show three new transitions of energies 211.2, 264.1, and 297.5 keV. In the spectrum gated on the new 278.1-keV transition and the 952.4-keV transition in ^{134}I (the 1133.8-keV transition in ^{135}I), one sees the same new transition of energy 211.2 keV, besides a new 324.5-keV transition. The spectra gated on the new 195.9- and 264.1-keV transitions, the new 195.9- and 211.2- keV transitions, and the new 278.1- and 324.5-keV transitions show the other new transitions and the coincidence relationships among these new transitions and those known ones in $^{133-136}$I. These data enable us to establish a new level scheme belonging to one Rh isotope, as shown in Fig. 6. A method, which has been successfully used for our work in ^{134}I, ^{139}Cs, ^{140}Cs, ^{142}Cs [51-54], was adopted to determine the mass number of the present level

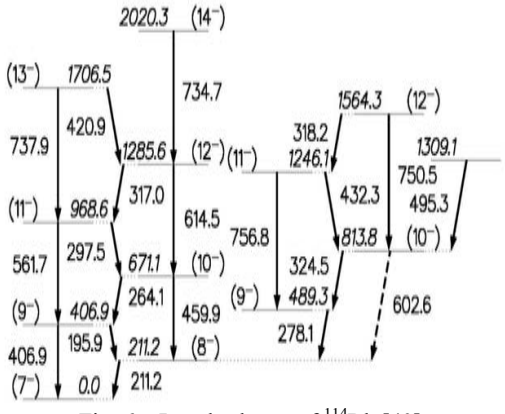

Fig. 6 – Level scheme of ^{114}Rh [40].

scheme. In the 279.7/224.8- (^{111}Rh), 60.6/183.0- (^{112}Rh), 232.2/240.6- (^{113}Rh), and 195.9/264.1-keV double gates, the fission yield ratios of the 1111.8-keV transition in ^{136}I to the 1133.8-keV transition in ^{135}I were measured to be 0.80(11), 0.55(8), 0.32(4), and 0.21(3), respectively. The variation of these ratios follows those of ^{142}Cs to ^{141}Cs in the $^{105-108}$Tc gates. So it is reasonable to assign the mass number 114 to the level scheme we established. The spin-parity assignments to the levels in the level scheme of ^{114}Rh as shown in Fig. 6 are mainly based upon the analogy with the level structures of the lighter Rh isotopes.

The level scheme of ^{115}Rh established in the present work is shown in Fig. 7. One clearly sees that the energy of the strongest transition in ^{115}Rh is very close to the strongest 211.7-keV transition in ^{111}Rh and ^{113}Rh [32] with much larger fission yields than ^{115}Rh and the 211.2-keV transition in ^{114}Rh [40]. So one highlight of the present work is the separation of the four peaks, the 211.7 keV in ^{111,113}Rh, the 211.2 keV in ^{114}Rh, and the 213.3 keV in ^{115}Rh, in the spectra with gates set on transitions in their iodine partners. The identifications of the transitions in ^{115}Rh were based on extensive cross-checking of the coincidence relationships and relative intensities among transitions in its complementary fission fragments $^{133-135}$I [55,27,51] and itself. Careful background subtractions were always performed to eliminate possible accidental coincidences. Several coincidence spectra were created by double-gating on strong transitions in $^{133-135}$I and new ones assigned to ^{115}Rh to show evidence for the identifications of new transitions in ^{115}Rh. Two spectra were obtained by double-gating on two transitions in ^{134}I and ^{135}I, where a new transition of energy 247.7 keV is seen in both spectra, along with the previously known strong transitions in $^{111-114}$Rh [32, 42, 40]. Three spectra were obtained by double-gating on the new 247.7-keV transition and a strong transition in each of ^{133,134,135}I, respectively. Two new transitions of energies 213.3 and 242.2 keV are seen in these spectra. The 211.7-keV transition in ^{113}Rh and the new 213.3-keV transition form a doublet peak because of the large fission yield of ^{113}Rh, the 4n fission partner of ^{135}I. The spectra gated on the new 213.3-keV transition and on the 912.7- (^{133}I), 952.4- (^{134}I), and 1133.8- keV (^{135}I) transitions, respectively, clearly demonstrate the coincidence relationships among the new 213.3-, 242.2-, and 247.7-keV transitions as well as those in the I isotopes. One new transition of energy 489.9 keV, equal to the sum of 242.2 and 247.7 keV, is

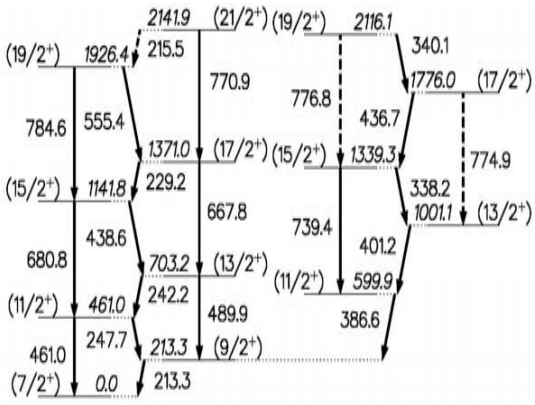

Fig. 7 – Level scheme of ^{115}Rh[45].

coincident with the 213.3-keV transition. A new transition of energy 386.6 keV is observed in Fig. 7, but not coincident with the new 247.7-keV transition. So the new 386.6-keV transition, in coincidence with the new 213.3-keV transition and the transitions in the I isotopes, should be in another band in this Rh nucleus, which is supported by observing the 213.3.-keV transition and two new transitions of energies 338.2 and 401.2 keV in the spectra double-gated on the new 386.6-keV transition and on the 912.7- (^{133}I), 952.4- (^{134}I), and 1133.8-keV (^{135}I) transitions. Three spectra gated on the new 213.3- and 247.7-keV transitions, the new 242.2- and 247.7-keV transitions, and the new 386.6- and 338.2-keV transitions, respectively, indicate the coincidence relationships among the newly observed transitions and known ones in $^{133–135}$I. These coincidence data enable us to establish a new level and assign it to a single Rh isotope, as shown in Fig. 7.

As seen in the above spectra, the transitions in the level scheme shown in Fig. 7 are in coincidence with transitions in I isotopes. Therefore, we proposethat the level scheme in Fig. 7 belongs to ^{115}Rh since the level schemes of $^{111–114}$Rh are already known. The most crucial support comes from the following measurements to determine the mass number of these transitions. In the 60.6/183.0- (^{112}Rh), 232.2/240.6- (^{113}Rh), 195.9/264.1- (^{114}Rh), and 213.3/247.7-keV double gates, the fission yield ratios of the 1133.8-keV transition in ^{135}I to the 952.4-keV transition in ^{134}I were measured as 13.9(19), 5.63(79), 3.80(53), and 1.92(27), respectively. The variation of these ratios is very similar to those of ^{142}Cs to ^{141}Cs in the $^{105–108}$Tc gates. Therefore, we conclude that the (247.7 → 213.3)-keV cascade is in ^{115}Rh after considering the fact that the fission yield of ^{115}Rh is much greater than those of other heavier Rh isotopes in the ^{252}Cf fission. The same ratio in the 213.3/386.6-keV gate was also measured to be 1.97(28), which is consistent with the value in the 213.3/247.7-keV gate. So the (401.2 → 386.6)-keV cascade forms a sideband in ^{115}Rh, as shown in Fig. 6. Because of the severe overlap of the 211.7-keV transition in ^{113}Rh and the 211.2-keV transition in ^{114}Rh and weak population of ^{115}Rh in the ^{252}Cf fission, only γ branching ratios for some levels were measured instead of the relative transition intensities.

3. DISCUSSION

3.1. ^{118,120,122}Cd

For even-N Cd isotopes the even-parity states can be generated by two quasi-proton states of $(\pi g_{9/2})^{-2}$, $(\pi p_{1/2})^{-2}$ and/or two quasi-neutron states $(\upsilon h_{11/2})^2$, $(\upsilon d_{3/2})^2$, or $(\upsilon s_{1/2})^2$, the odd-parity states by two quasi-proton states $(\pi g_{9/2}\pi p_{1/2})^{-2}$ or two quasi-neutron states $(\upsilon s_{1/2}\upsilon h_{11/2})$, $(\upsilon d_{3/2}\upsilon h_{11/2})$, $(\upsilon g_{7/2}\upsilon h_{11/2})$. Odd-parity levels with spin ranging from one to nine are expected to occur as seniority-2 states in even-N Cd isotopes. We tentatively assign a configuration of two quasi-protons $(\pi g_{9/2})^{-2}$ and two quasi-neutrons $(\upsilon h_{11/2})^2$ state to the excited members of the ground band in

^{118,120}Cd, the former (and the coupling with the latter) form the levels up to 8^+, and the latter (and the coupling with the former) may generate the levels with spins higher. The quasi-rotational alignment of $(\upsilon h_{11/2})^2$may explain the very sharp quasi-rotational back-bending of the bands (see below).

We assign a mix of two-quasi-proton states $(\pi g_{9/2}\pi p_{1/2})^{-2}$, and two quasi-neutron states $(\upsilon h_{11/2}\upsilon d_{3/2})$, $(\upsilon h_{11/2}\upsilon s_{1/2})$ to the 2223.2 keV, 5^- level in ^{118}Cd and the 2129.1 keV, 5^- level in ^{120}Cd, although some authors have assigned quadrupole-octupole coupled $2^+ \times 3^-$ state to the 5^- level in lighter even-N Cd isotopes. This quadrupole-octupole coupled (QOC) state is not likely a reasonable assignment for the 5^- level in ^{118,120}Cd, since the expected levels (quintuplet) associated with the $2^+ \times 3^-$ coupling are not observed in these heavier Cd isotopes. And, as a matter of fact, as pointed by Garrett and Wood [19], the re-study of ^{112}Cd by single-nucleon-transfer reaction ^{111}Cd(d,p) using polarized deuteron beams concluded that the wavefunction must be dominated by the $(\upsilon h_{11/2}\upsilon s_{1/2})$ two-quasineutron configuration, in disagreement with the assignment as a member of the QOC quintuplet, which would require that the wavefunction be dominated by four-quasi-particle amplitudes. The 2640.4 keV, 7^- level in ^{118}Cd may originate from the two quasi-neutron configuration $(\upsilon d_{3/2}\upsilon h_{11/2})$ or $(\upsilon g_{7/2}\upsilon h_{11/2})$.

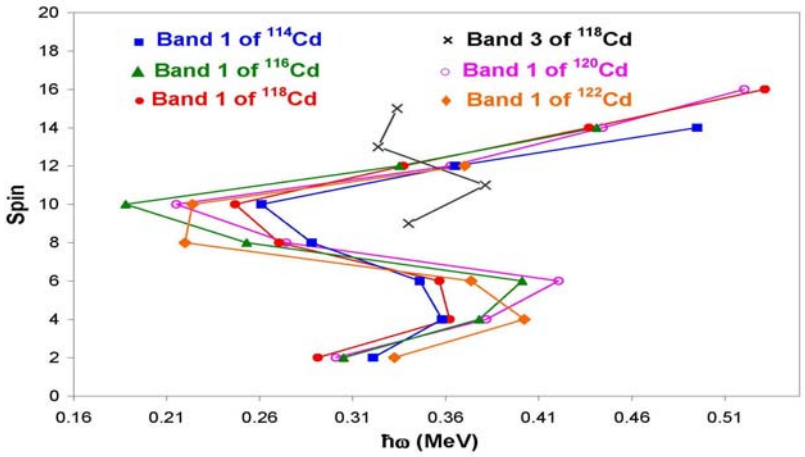

Fig. 8 – A model-independent plot of level spin versus ħω for the ground band 1 in even-N isotopes $^{114\text{-}122}$Cd[28].

As mentioned in the introduction section, there have been many competing theoretical explanations for the excited levels of the even- N Cd nuclei. Let us make clear from the outset that there is no absolute determination of a particular nuclear model for these states. There are many representations that can describe the nuclear states; it is mainly a question of which representation can describe the nuclear properties with the fewest terms in an expansion. For cadmium, only two

protons less than the closed shell Z=50, it was long considered that there should be spherical ground states. Also the ground band and side bands were long considered the best examples of quadrupole vibrations about a spherical minimum. As experiments showed more than one 0^+ state at energies where 2-phonon vibrational states should be, then it was necessary to invoke "intruder states". Furthermore, B(E2) values did not fit the model of spherical vibrational states of one, two, or three quadrupole vibrational phonons. Interacting-boson models have been developed and applied also, giving the spherical vibrational models a microscopic basis but not gaining a universal acceptance [19]. There have also been Hartree-Fock + BCS calculations of $^{113\text{-}116}$Cd showing ground-state prolate spheroidal minima, especially for the odd-A isotopes [22].

There seems to be no consensus at present about the "vibrational" or "shape-rotational" models in this region of cadmium nuclei. Garrett and Wood [19] pointed out that energy patterns alone can be very misleading for isotopes like $^{110\text{-}116}$Cd which appear, on the basis of low-lying excitation energies, to be beautiful examples of harmonic quadrupole vibrations. Vibrational nature is found to be refuted in the Cd isotopes; and experimental data seriously contradict a vibrational interpretation in deformed nuclei. Rather than present kinematic moments of inertia or alignment plots of the yrast data, we show in Fig. 8 a model-independent plot of level spin versus ħω, such as that used by Frauendorf, Gu, and Sun in their recent paper "Tidal Waves: a non-adiabatic microscopic description of the yrast states in near-spherical nuclei" [56], for the ground bands of even-N $^{114\text{-}120}$Cd. In [40] the Shell Correction version of the Tilted Axis Cranking model (SCTAC) was used to study the tidal waves, that run over the nuclear surface, in the nuclei with even-Z =44-48 and even-N=56-66. In Fig. 5 of ref. [56], theoretical J ~ ħω (β ranging from 0.1 to 0.2 and $\gamma=10^0$-15^0) was compared to experimental values of the ground bands of $^{104\text{-}114}$Cd, and good agreement was achieved, which implies triaxial deformations also in these even-N Cd isotopes. Based on the present new level schemes the spin versus ħω curves for even-N ^{118,120}Cd and ^{116}Cd shown in Fig. 8 all exhibit a similar variation, as seen in ^{114}Cd, showing evidence for triaxial deformations in ^{116,118,120}Cd. The cure for band 3 observed in ^{118}Cd shows similar feature. In addition, the observations that the excitation of the second 2^+ level is only slightly higher than that of the 4^+ level in the ground band are consistent with this conclusion. The sharp back-bending of the spin versus ħω curves in the ground bands in $^{114\text{-}120}$Cd, are similar to those in $^{106\text{-}114}$Cd shown in Fig. 5 of ref. [56]. According to the discussion for weakly deformed nuclei by Frauendorf *et al.*, [56], the sharp back-bending is caused by the quasi-rotational alignment of a pair of $h_{11/2}$ neutrons. The sharpness of the back-bending depends sensitively on the position of the neutron chemical potential λn relative to the $h_{11/2}$ level [56].

By using the transition energies E_γ and branching ratios $I\gamma(E1)/I\gamma(E2)$ determined, the B(E1)/B(E2) (10^{-6} fm^{-2}) ratios of the levels of odd-parity band 2 in ^{118,120}Cd were calculated according to the equation

$$B(E1)/B(E2) = 0.771[E\gamma(E2)5\ I\gamma(E1)]/[\ E\gamma(E1)3\ I\gamma(E2). \quad (1)$$

The B(E1)/B(E2) ratios range from 0.012 to 1.83 (10^{-6} fm^{-2}) in the even-N ^{118,120}Cd. The B(E1)/B(E2) ratios determined for the new band 2 built on the 5^- state in ^{118,120}Cd show small differences in the center-of-mass and center-of-charge (electric dipole moment) in these Cd isotopes.

Wang *et al.* [8] obtained the gamma transition branching ratios from the beta decay work. With the large mixture of isotopes in our data, we cannot improve upon their measurements. However, we note here that the relative decay to ground from the second 2^+ states are much weaker than they would be from a spheroidal nucleus with good K quantum number of 2. For this effect see the detailed analysis of Os isotopes by Allmond *et al.* [57].

3.2. ^{114,115}Rh

Earlier investigations of odd-odd Rh isotopes in decay studies established their low-lying excited states. The ground states of odd-odd $^{104-114}$Rh were found to have a spin-parity of 1^+ [58]. High-spin states of negative parity in ^{104,106,108,110,112}Rh have been established built on their isomeric states [32, 36-38]. A 6^+ isomeric state was proposed for ^{106,112}Rh while a 5^+ isomeric state was proposed for ^{104,108,110}Rh [5, 9–11]. Note that the 7^- states of the I = 1, negative-parity bands of odd-odd $^{104-112}$Rh decay either to the 5^+ (or 6^+) isomeric state through a 6^- state or directly to the 6^+ isomeric state. One observes a remarkable likeness between the level structures of ^{110}Rh and ^{112}Rh relative to the 7^- state and also their resemblance to the level structure of ^{114}Rh. Therefore, it is reasonable to propose that the high-spin level scheme of ^{114}Rh is built on a 7^- state with the $\pi g_{9/2} x \nu h_{11/2}$ configuration, which is solidified by the theoretical calculations presented later. However, we have not observed any transition depopulating the 7^-state in ^{114}Rh to an isomeric state. Note that in the case of ^{112}Rh the $7^- \rightarrow 6^+$ transition has a small transition energy of 60.6 keV.

The signature is a quantum number associated with the invariance of a system with an intrinsic quadrupole deformation under a rotation of 180^0 around a principal axis [59]. Due to this symmetry, level energies E(I) of a high-j rotation band are split into two branches with $\Delta I = 2$, classified by the signature quantum number. The signature splitting is a measure of the difference of the Routhians (the energy referring to the rotating coordinate system) between the two signature branches of a rotation band. This quantity can be used as an indicator of the shape of a nucleus. Triaxial deformations can contribute to a large signature splitting, because K is not a good quantum number any longer. If the Routhian of the favored signature is found to lie higher in energy as compared to that of the unfavored one, the corresponding signature splitting is anomalous. The signature splitting becomes normal at some spin where signature inversion occurs.

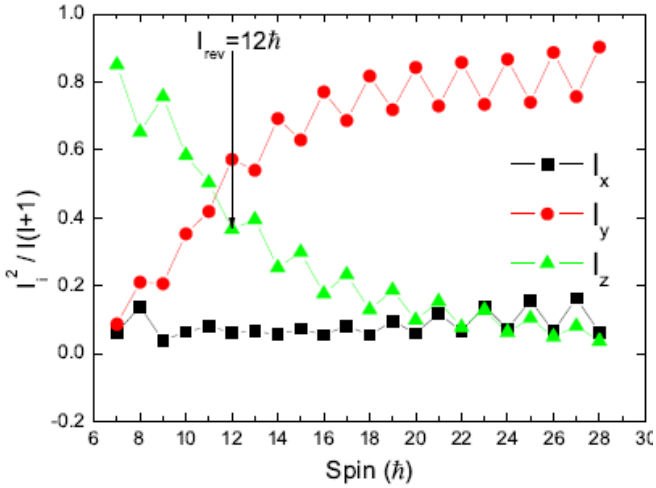

Fig. 9 – Calculated expectation values of I_x^2, I_y^2 , and I_z^2 in unit of I(I +1) with the wave functions from a diagonalization that has reproduced the ^{114}Rh experimental data [40].

In the E(I)−E(I −1)(energy difference) vs spin plot for the yrast band of ^{114}Rh, one clearly sees E(I)−E(I −1) in the favored signature branch is located above that in the unfavored signature branch at low spins. The energy differences in the favored signature branch are lower than those in the unfavored branch after I =12, where the signature inversion occurs. After that, the signature splitting becomes normal and the anomalous splitting disappears. The observation of the anomalous signature splitting and the signature inversion is a common feature in many mass regions, A = 80,100,130,160.

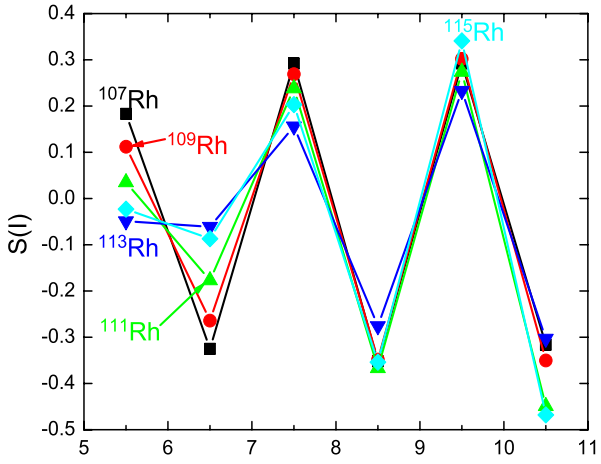

Fig. 10 – Signature splitting function S(I) vs spin for the yrast bands of odd-even $^{107-115}$Rh. Data are taken from Refs. [35, 32, 41] and the present work [45].

To probe the character of the rotational motion of the triaxially shaped nucleus ^{114}Rh, calculations have been carried out for the expectation values of three components of the total angular momentum along the principal axes by using the TPSM wave functions from diagonalization that has reproduced the experimental data well, as seen in Fig.9. The tri-axially deformed single-particle states for ^{114}Rh are generated by the Nilsson Hamiltonian with the deformation parameters $\varepsilon_2 = 0.253$ and $\gamma = 32$ (Lund convention), which are supported by Total Routhian Surface calculations. Three major shells, N = 3, 4, and 5, are considered each for neutrons and protons. The level energies E(I) of the $\pi g_{9/2} x h_{11/2}$ yrast band in ^{114}Rh have been calculated up to I = 28, and the experimental level energies are well reproduced. It is suggested that the observed signature reversion be attributed to the change of the rotational mode, from the quasi-particle aligned rotation to the collective rotation. At low spins, the angular momentum is mainly built by the alignments of the last $h_{11/2}$ neutron and $g_{9/2}$ proton, while being in competition with strong collective rotation, so the situation is somewhat complicated. At spins larger than 12, the signature splitting has its normal phase and increases with increasing spins, and these are indeed the characteristics of the collective rotation, or principal axis rotation.

It is worth mentioning that the present work is the first investigation of the signature inversion in neutron-rich A ~ 110 isotopes, which has opened up new challenges to both experiment and theory. This work extends the application of the triaxial projected shell model from the A = 130 region [60] to the A = 110 region as the mechanism of the signature inversion. Note that the studies in Ref. [60] indicate the impact of the residual proton-neutron interactions merely modifying the position of the reversion spin. Further work on systematic studies of the signature inversion in lighter Rh isotopes as well as in Ag isotopes in this mass region is in progress.

The level structure of ^{115}Rh, as presented in Fig. 7, bears significant resemblance to bands 1 and 6 of ^{107,109}Rh [41,42] and ^{111,113}Rh [32, 42] that are built on the $\pi g_{9/2}$ subshell. The identified levels in ^{115}Rh do not reach such high spins as those in ^{111}Rh and ^{113}Rh; only two bands were observed in ^{115}Rh, fewer than in ^{107,109,111,113}Rh. We proposed that the present level scheme of ^{115}Rh is built on the $7/2^+$ ground state and we assigned spin parities to other higher levels based on systematics and their yrast and high-spin features. A sideband strongly populating the yrast $9/2^+$ excited level has been observed in ^{115}Rh, as in ^{107,109,111,113}Rh, whose features indicate a deviation from axial symmetry. $11/2^+$ was assigned to its bandhead and $13/2^+$, $15/2^+$, $17/2^+$, and $19/2^+$ to other higher states. In Ref. [26], the study on ^{125}Xe shows that the signature pattern of the yrast band could appear in two triaxial shapes, on either the prolate or the oblate side. The sideband, the so-called yrare band, can be used to determine on which side is the triaxial shape. The sideband in the Xe isotope is analogous to the sideband here in ^{115}Rh, as confirmed in ^{111,113}Rh in Ref. [32].

The signature splitting of ^{115}Rh is basically comparable to those of ^{107,109,111,113}Rh. The plots for the signature splittings in the yrast bands of odd-even $^{107–115}$Rh are presented in Fig. 10. Such large signature splittings observed in ^{107,111,113}Rh have been interpreted in Refs. [32,41] in terms of triaxiality playing amajor role. the signature splitting in ^{113}Rh is seen as the smallest one among ^{107,109,111,113,115}Rh, while the γ value for ^{113}Rh is almost identical to the values for ^{111,115}Rh. We also noticed that calculations based on the RTRP model in Ref. [6] did produce a larger splitting than experiment with $\gamma = 28\circ$. Thus, an interesting open question emerges concerning the trends of the γ values with the signature splitting and increasing neutron numbers. The experimental excitation energies have been compared to the theoretical results based on the rigid triaxial rotor plus particle model, with good agreement. This model has successfully described the properties of neutron-rich odd-even Rh, Tc, Nb, and Y isotopes. The deformation parameters fitted to ^{115}Rh are $\varepsilon = 0.26$ and $\gamma = 27.5\circ$. The lowest yrast states are dominated by a K = 7/2 component. The intrinsic state is dominated by the particle projection quantum number $\Omega = 7/2$ all along the yrast band, and in the lower half of the yrare sequence. The lower-spin states of the yrare band are dominated by K = 11/2 components. The strong signature splitting in the yrast band is typical for triaxiality, and this feature is satisfactorily described by the model.

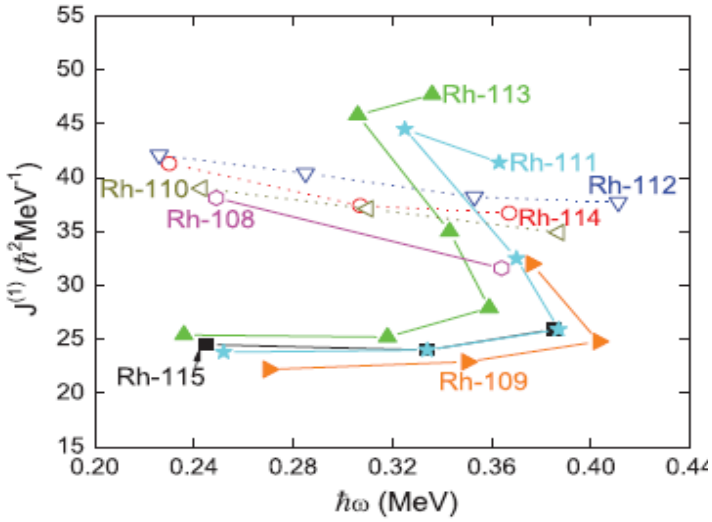

Fig. 11 – Kinetic moment of inertia vs frequency for the $\alpha = +1/2$ signature partners of the yrast bands of odd-even $^{108–115}$Rh and the even-integer signature partners of the yrast bands of odd-odd $^{108–115}$Rh. Backbending is observed in ^{109,111,113}Rh. Data are taken from Refs. [32,40,37] and the present work [45].

In Ref. [32], Luo *et al.* reported the observation of backbending in the yrast bands of ^{111,113}Rh that sets in above the $21/2^+$ level in ^{111}Rh and the $19/2^+$ level in ^{113}Rh. Therefore, it is of interest to find if the backbending occurs in ^{115}Rh. The

backbending plot (kinetic moment of inertia *vs* rotational frequency) was investigated for the yrast bands of $^{108–115}$Rh as shown in Fig. 11. A backbending was clearly seen in ^{109}Rh, ^{111}Rh, and ^{113}Rh and the backbending frequency moves monotonically higher with decreasing neutron numbers. For ^{115}Rh, its kinetic moment of inertia at low rotational frequency is comparable to those for ^{109}Rh, ^{111}Rh, and ^{113}Rh. One cannot determine where a backbending occurs in ^{115}Rh because levels in ^{115}Rh identified here are not as high as in ^{109,111,113}Rh. However, one may predict that the backbending frequency in ^{115}Rh, which is obviously higher than that in ^{113}Rh, is either comparable to or higher than that in ^{111}Rh or higher than even that in ^{109}Rh. It is very interesting to see that the backbending in ^{115}Rh does not conform to the above systematics in ^{109}Rh, ^{111}Rh, and ^{113}Rh, where the backbending frequency systematically decreases in going from ^{109}Rh to ^{113}Rh. More experimental work is needed to find the accurate backbending frequency and further theoretical work is required to interpret the above observation if it is correct. Data for the odd-odd $^{108–114}$Rh are also included in Fig. 11, where no backbending is found. The lack of backbending in ^{108,110,112,114}Rh could be due to blocking by the odd neutron. So the backbending in ^{109}Rh, ^{111}Rh, and ^{113}Rh means a neutron pair breaking in these odd-even Rh isotopes. As mentioned in Ref. [45], the breaking pair is in the $h_{11/2}$ neutron orbital.

4. SUMMARY

The present study provides evidence that both the spherical shell-model quasi-particle/hole couplings and quasi-rotational degrees of freedom are playing roles in these Cd isotopes which have two quasi-proton holes in the Z=50 major shell closure and cover the range of N from 69 through 72, mostly near the half-filled $h_{11/2}$ neutrons. Triaxiality is probable in these Cd isotopes. The difference in variations of spin ~ ħω of the yrast bands between the even-N Cd isotopes and the odd-N Cd ones may indicate the role of the quasi-rotational alignment of the $(\upsilon h_{11/2})^2$ neutron pair and the blocking effect of the odd $h_{11/2}$ neutron. The B(E1)/B(E2) ratios determined for the levels of the side bands are small, showing small differences in the center of mass and center of charge in these Cd isotopes as well.

The present work established high-spin level schemes of ^{114,115}Rh for the first time. The level scheme in ^{114}Rh bears a remarkable similarity to those of lighter Rh isotopes. The signature inversion was observed in the yrast band of ^{114}Rh. We assigned spins and parities to levels in the yrast band which has a configuration of $\pi g_{9/2} x \nu h_{11/2}$. A side-band was found to feed the yrast 8^- state indicating triaxiality playing a role in the structure of ^{114}Rh. The signature inversion was observed in the yrast band of ^{114}Rh with I_{rev} = 12. The triaxial projected shell model was used to interpret the signature inversion in ^{114}Rh. Model calculations successfully predicted

I_{rev} = 12 and reproduced the experimental level energies in ^{114}Rh very well. Further examinations showed that the change of the rotational mode from quasi-particle aligned rotation to collective rotation can give rise to signature inversion in ^{114}Rh.

A large signature splitting is observed in the yrast band of ^{115}Rh. The previous and present studies in odd-even Rh isotopes with triaxiality show that triaxiality increases from ^{107}Rh to ^{111}Rh and then remains much the same for ^{113,115}Rh. Systematic studies of neutron-rich even-N Ru, Rh, and Pd isotopes indicate an N = 68 effect where the nucleus has the lowest excitation energies. This phenomenon is seen in the yrare bands in odd-even Rh as well. A large signature splitting is observed in the yrast band of ^{115}Rh by plotting the signature splitting function S(I), which follows the systematics that large signature splittings have been found in lighter odd-even Rh isotopes from A = 107 to A = 113. A small but inverted signature splitting in the yrare band is observed. The experimental excitation energies have been compared to the theoretical results based on the rigid triaxial rotor plus particle model, with good agreement. This model has successfully described the properties of neutron-rich odd-even Rh, Tc, Nb, and Y isotopes. The deformation parameters fitted to ^{115}Rh are $\varepsilon = 0.26$ and $\gamma = 27.5^{\circ}$. The lowest yrast states are dominated by a K = 7/2 component. The intrinsic state is dominated by the particle projection quantum number K = 7/2 all along the yrast band, and in the lower half of the yrare sequence. The lower-spin states of the yrare band are dominated by K = 11/2 components. This high value of K is connected to a shift of the rotational angular momentum toward a principal axis with a lower moment of inertia. Also the strong signature splitting in the yrast band is typical for triaxiality, and this feature is satisfactorily described by the model. Themeasured γ branching ratios have been satisfactorily described by the model, which reflect the core structure of the wave functions.

Acknowledgments. The work at Vanderbilt University and Lawrence Berkeley National Laboratory was supported by the U.S. DOE Grants DE-FG-05-88ER40407 and DE-FG02-95ER40934, respectively.

REFERENCES

1. B. Rosner, Phys. Rev. B**136**, 644 (1964).
2. G. E. Gordon, Phys. Rev. B**136**, 618 (1964).
3. Y. Kawase *et al.*, Nucl. Phys. A**241**, 237 (1975).
4. B. Fogelberg *et al.*, Nucl. Phys. A**267**, 317 (1976).
5. B. Fogelberg *et al.*, Phys. Lett. **36**B, 334 (1971).
6. A. Aprahamian *et al.*, Phys. Rev. Lett., **59**, 535 (1987).
7. H. Mach *et al.*, Phys. Rev. Lett. **63**, 143 (1989).
8. Y. Wang *et al.*, Phys. Rev. C67, 064303 (2003).
9. N. Hoteling *et al.*, Phys. Rev. C76, 044324 (2007).
10. S. Drissi *et al.*, Nucl Phys. A614, 137 (1997).
11. P.E. Garrett *et al.*, Phys. Rev. C59, 2455 (1999).

12. A. Gade and P. von Brentano, Phys. Rev. C66, 014304 (2002).
13. D. Bandyopadhyay *et al.*, Phys. Rev. C67, 034319 (2003).
14. J.C. Batchelder *et.al.*, Phys. Rev. C80, 054318 (2009).
15. F. Corminboeuf *et al.*, Phys. Rev. C63, 014305 (2000).
16. J. Meyer-Ter-Vehn, Nucl. Phys. A249, 111 (1975).
17. J. Meyer-Ter-Vehn, Nucl. Phys. A249, 141 (1975).
18. S. Ohya *et al.*, Nucl. Phys. A334, 382 (1980).
19. P.F. Garrett and J.L. Wood, J. Phys. G37, 064028 (2010).
20. N. Fotiades *et al.*, Phys. Rev. C**61**, 064326-1 (2000).
21. N. Fotiades *et al.*, Physica Scripta, T**88**, 127 (2000).
22. N. Buforn *et al.*, Eur. Phys. J. A**7**, 347 (2000).
23. J.K. Hwang *et al.*, J. Phys. J**28**, L9 (2002).
24. Shu-Dong Xiao *et al.*, Chinese Journal High Energy Phys. and Nucl. Phys. 28, 37 (2004).
25. Clarke Nelson, Senior Honors Thesis, Vanderbilt University, 2010.
26. J.H. Hamilton *et al.*, Prog. Part. Nucl. Phys. **35**, 635(1995).
27. C.T. Zhang *et al.*, Phys. Rev. Lett. **77**, 3743(1996).
28. Y.X. Luo *et al.*, submitted to Nucl. Phys. **A** (2010), and revised (2011).
29. H. Mach *et al.*, Phys. Lett. B 230, 21 (1989).
30. J. Skalski, S. Mizutori, and W. Nazarewicz, Nucl. Phys. A617, 282 (1997).
31. H. Hua, *et al.*, Phys. Rev. C 69, 014317 (2004).
32. Y. X. Luo *et al.*, Phys. Rev. C 69, 024315 (2004).
33. Y. X. Luo *et al.*, Phys. Rev. C 70, 044310 (2004).
34. Y. X. Luo *et al.*, J. Phys. G: Nucl. Part. Phys. 31, 1303 (2005).
35. Y. X. Luo *et al.*, Phys. Rev. C 74, 024308 (2006).
36. R. Duffait *et al.*, Nucl. Phys. A454, 143 (1986).
37. N. Fotiades *et al.*, Phys. Rev. C 67, 064304 (2003) and references therein.
38. P. Joshi *et al.*, Phys. Lett. B 595, 135 (2004).
39. A. Jokinen *et al.*, Nucl. Phys. A549, 420 (1992).
40. S. H. Liu *et al.*, Phys. Rev. **C 83**, 064310 (2011).
41. Ts. Venkova *et al.*, Eur. Phys. J. A **6**, 405 (1999).
42. Ts. Venkova *et al.*, Eur. Phys. J. A **15**, 429 (2002).
43. J. Kurpeta *et al.*, Eur. Phys. J. A **31**, 263 (2007).
44. J. ÄystÖ *et al.*, Phys. Lett. B **201**, 211 (1988).
45. S.H. Liu *et al.*, Phys. Rev. **C 84**, 014304 (2011).
46. A.M. Baxter *et al.*, Nucl. Inst. Meth. **A317**, 101 (1992).
47. D.C. Radford, Nucl. Inst. Meth. **A317**, 297(1995), also cf. his website http://radware.phy.ornl.gov/
48. A. Daniel *et al.*, Nucl. Inst. Meth., B262, 399 (2007).
49. P.E. Haustein *et al.*, Nucl. Data Tables, A10, No. 4 – 5, 321 (1972).
50. H.W. Taylor *et al.*, Nucl. Data Tables, A9, 1 (1971).
51. S. H. Liu, *et al.*, Phys. Rev. C 79, 067303 (2009).
52. S. H. Liu *et al.*, Phys. Rev. C 80, 044314 (2009).
53. S. H. Liu *et al.*, Phys. Rev. C 81, 037302 (2010).
54. S. H. Liu *el al.*, Phys. Rev. C 81, 057304 (2010).
55. W. B. Walters, E. A. Henry, and R. A. Meyer, Phys. Rev. C **29**,991 (1984).
56. S. Frauendorf, Y. Gu, and J. Sun, Inter. Jour. of Modern Phys. E20, 465 (2011).
57. J.M. Allmond *et al.*, Phys. Rev. C78, 014302 (2008).
58. http://www.nndc.bnl.gov/ensdf/
59. A. Bohr and B. R. Mottelson, Nuclear Structure (W. A. Benjamin, Inc., New York, 1975), Vol. II.
60. Z. C. Gao, Y. S. Chen and Y. Sun, Phys. Lett. B 634, 195 (2006).